Journal of Computational Applied Mechanics 2026, 57(3): 514-525

DOI: 10.22059/jcamech.2026.409534.1765

RESEARCH PAPER

The intricate link between anterior cruciate ligament rupture and lower limb muscle fatigue, Musculoskeletal Modeling

Zeynab Saghaeinooshabadi [a], Mohammad Reza Zakerzadeh [a], Mohammad Ali Nazari [a, b,*]

[a] *School of Mechanical Engineering, College of Engineering, University of Tehran, Tehran, Iran*
[b] *Université Grenoble Alpes, CNRS, Grenoble INP, TIMC, Grenoble, France*

Abstract

Objective: Anterior Cruciate Ligament (ACL) rupture can independently affect an individual's quality of life. This impact becomes more significant when fatigue and intense activity are involved. The aim of this study is to investigate the muscle forces generated in various muscles of the healthy and injured leg using musculoskeletal modeling in OpenSim software.
Methods: In this study, a participant with unilateral ACL rupture was asked to perform a one-hour walking protocol. Kinematic data were recorded using reflective markers and motion capture cameras, while kinetic data were collected via force plates. These data were used to model the gait and calculate muscle forces in different leg muscles using full inverse analysis workflow. Notable differences were observed in muscle forces between the healthy and injured legs. These differences were particularly evident in the Semimembranosus, Soleus and Gracilis muscles. The Vastus Medialis and Vastus Intermedius of the injured leg produced up to 30% more force compared to the corresponding muscles in the healthy leg during the gait cycle, while the Soleus muscle in the healthy leg generated 47% to 74% greater force Relative to the contralateral limb. The Gracilis muscle also showed more than 45% difference in force production favoring the injured leg. Dynamic musculoskeletal modeling was used as a more comprehensive method than surface electromyography for assessing different muscles even deep muscles in patients with musculoskeletal disorders. The results agree with EMG study for Vastus Medialis, Gastrocnemius Lateralis and Soleus. Gastrocnemius Medialis showed an approximate agreement with IEMG (Integrated Electro MyoGraphy) results. The behavior of the other surface muscles does not comply with IEMG results. This shows that a better modeling which includes the ligaments is needed.

Keywords: Musculoskeletal modeling; Anterior Cruciate Ligament injury; OpenSim; muscle fatigue; Inverse kinematics and dynamics; Gait analysis; Computed muscle control

1. Introduction

Assessing the level of fatigue in various fields, including sports, occupational, and rehabilitation activities, has always been of great importance. This assessment can play an effective role in analyzing the nature of the activity, optimizing task design, and generally in measuring the degree of match between task demands and the individual's functional capacity [1, 2]. The persistence of muscle fatigue and its consequences, such as muscle pain [3] or loss of functional capacity, are among the fundamental challenges in fields such as rehabilitation, human resource management, and occupational health and safety [4]. Fatigue can increase the likelihood of accidents and seriously affect the quality of performing tasks that require high precision [1, 5].

Various studies have shown that muscle fatigue is associated with changes in electromyographic signal specifications, such as Median Frequency (MDF) or Integrated Electromyography (IEMG) or Root Mean Square (RMS) [6-12]. These changes can be used as indicators for diagnosing and measuring fatigue. On the other hand, estimating internal muscle forces through modeling will be of great importance in rehabilitation techniques and recovery of lost muscle strength, improving the quality and optimizing the sports performance of athletes [13, 14] , and preventing sports injuries or re-injury in professional athletes. Since it is difficult to directly measure muscle forces inside the body, musculoskeletal modeling has been proposed as an effective method for estimating these forces during movement. Several software tools have been developed in this field, among which the open-source software OpenSim is one of the most popular for simulating human movements, especially walking [15].

The knee joint, which plays an important role in walking, has been widely studied in human body simulations. As one of the most complex joints in the human body, the knee is associated with multiple bones, muscles, ligaments, and tendons. Among the various injuries affecting this joint, Anterior Cruciate Ligament (ACL) rupture is particularly prevalent. The ACL and Posterior Cruciate Ligament (PCL) primarily function to constrain the anteroposterior translation of the tibia relative to the femur. The ACL, which is biomechanically weaker than the PCL, plays a key role in preventing excessive anterior displacement of the tibia. Positioned at the center of the knee joint and intersecting in an oblique, X-shaped configuration, these two ligaments are fundamental to maintaining the mechanical stability and functional integrity of the knee [16].

A biomechanical analysis of the gait cycle in individuals with ACL injuries is among the most extensively investigated topics in the field. The gait cycle is the set of movements that begins when one foot contacts the ground and ends when the same foot contacts the ground again. A complete gait cycle is referred to as a stride [17]. Since muscles have the ability to increase or decrease the mechanical loads on the ACL, they are considered viable targets for preventive interventions [18]. Most studies that have measured muscle forces have focused on the effect of muscle fatigue on the risk of ACL injury [18-20], however, fewer studies have measured muscle forces in injured individuals.

In a previous study conducted by the authors [8], variations in EMG signal features were analyzed to examine muscle activity patterns in a person with ACL rupture subject to a fatigue exercise. Electromyographic electrodes were used to experimentally analyze the activity of healthy and injured leg muscles of the individual with ACL rupture, and muscle activity was assessed based on EMG data. To record muscle activity, wireless surface electrodes were used, which is a non-invasive method for recording muscle activity close to the skin surface. Surface electrodes made of Ag-AgCl were placed on the target muscles according to protocol proposed by the SENIAM standard [21]. After processing the EMG data recorded from three leg muscle groups, including quadriceps femoris, hamstrings, and triceps surae muscles, the changes in EMG features were analyzed as an indicator of muscle fatigue.

Despite its simplicity and usefulness in assessing muscle activity, the use of surface EMG is incapable of solving two problems: estimating the force produced in the muscles and the behavior of non-surface muscles. Therefore, calculating and estimating the force produced by different leg muscles and also investigating the behavior of non-surface muscles are among the issues that current research tries to answer using dynamic simulation software.

To quantify the muscle forces generated in both the healthy and injured legs of an individual with an ACL rupture during a prolonged walking protocol two primary data acquisition methods have been utilized: kinematic data obtained through the displacement of reflective markers tracked by motion capture cameras, and the kinetic data recorded via ground reaction forces measured by force plates embedded in the walkway. These datasets have been integrated within the OpenSim musculoskeletal modeling software [22] to compute muscle forces during gait. Subsequently, the estimated muscle forces in both the affected and unaffected legs have been analyzed and compared across various muscle groups to understand the biomechanical adaptations resulting from the ACL injury. The fatigue protocol procedure and the participant involved in the experiment are consistent with those reported in a previous study.

2. Materials and methods

In this section after an introduction of the modeling method in OpenSim, the experimental setup and the protocol for fatigue data collection is presented.

2.1. Musculoskeletal Modeling in OpenSim

OpenSim is an advanced, open-source software platform designed for dynamic modeling and simulation of the human musculoskeletal system. The software utilizes experimental data, such as marker trajectories captured from body-mounted markers and ground reaction forces recorded by force plates, to construct accurate and customizable models tailored to the anatomical characteristics of the individual under study[22]. The base model in OpenSim includes a set of virtual markers positioned anatomically analogous to the experimental markers. The scaling tool adjusts the anthropometry of the model to closely match the specific dimensions of the subject being tested [23].

After scaling the model to match the anthropometric dimensions of the individual participant in the inverse kinematics step, experimental marker coordinate data are input into the software, and joint positions and angles throughout the movement cycle are determined using a weighted least-squares approach. Following this, inverse dynamics computes the forces and moments acting on each joint based on Newtonian mechanics and the accelerations derived from the kinematic analysis. Finally, the residual reduction algorithm is employed to correct modeling errors and experimental data inconsistencies. [23].

Within OpenSim, two different primary methods are defined for estimating muscle-generated forces: Static Optimization (SO) and Computed Muscle Control (CMC). In SO, it independently optimizes muscle activation at each time step to satisfy the calculated joint moments for the known movement of the model. Conversely, CMC employs a proportional-derivative controller to adjust muscle excitations dynamically, minimizing the error between the current model state and experimental kinematics. At each time step, an instantaneous optimization problem is solved to determine the muscle excitations required to produce these accelerations [23, 24]. Using CMC method, following the workflow illustrated in Figure 1 the muscle-generated forces are estimated.

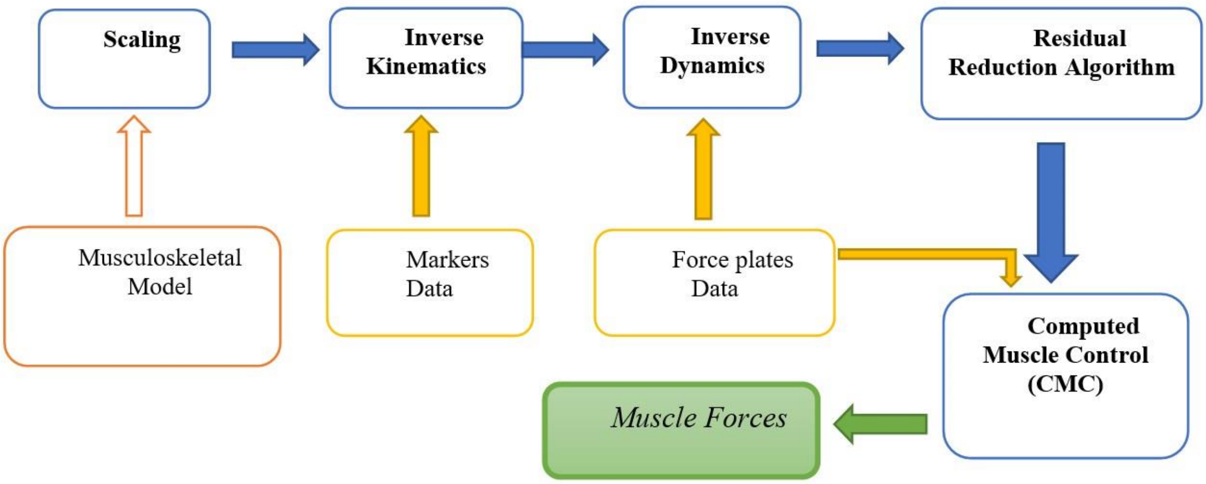

Fig 1: A schematic overview of the simulation workflow in OpenSim

In this study, the standard Gait2392 model—comprising 23 degrees of freedom and 92 musculotendon actuators—was employed to simulate the complex biomechanics of walking (Fig. 2). The input data consisted of body-mounted marker trajectories and ground reaction forces recorded via force plates.

2.2. Experimental Setup

As mentioned in the introduction, the test subject is the same individual who participated in the previous study [8]. A 42-year-old male patient (body mass: 77 kg, height: 172 cm) with a history of ACL rupture in his left knee. The subject had no other musculoskeletal disorders, had been injured in his left leg for about 4 years, and had not yet undergone ACL reconstruction surgery.

2.3. Marker Placement

For modeling in OpenSim software, it is necessary to attach reflective markers to specific anatomical landmarks on the body. In this study, the standard Plug-in Gait method was employed for lower limb marker placement. This method recommends installing markers on bony prominences and specific anatomical points of the body to record and simulate the movements of the skeleton and joints with the greatest accuracy [25]. Correct determination of these points is essential for defining the axes of joint movement and calibrating the movement model. In this method, markers were attached at the following points, bilaterally (Fig. 3):

- ASI: Placed directly over the anterior superior iliac spine.
- PSI: Placed directly over the posterior superior iliac spine.
- KNE: Placed on the lateral epicondyle of the knee.

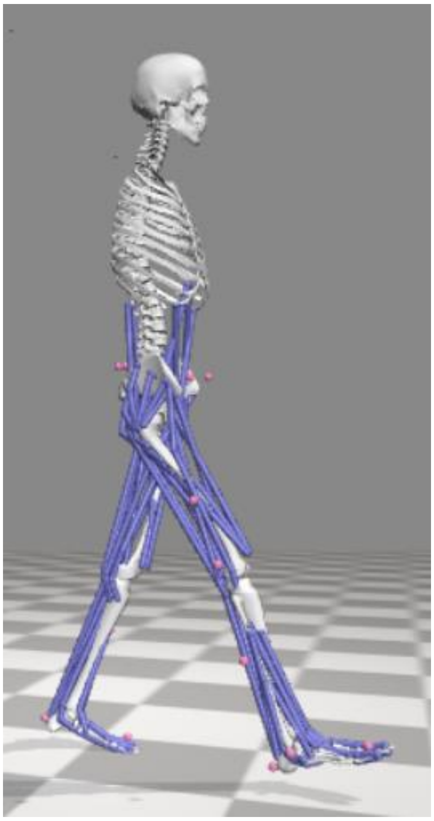

Fig 2: Customized musculoskeletal model within the OpenSim

Fig 3. The bright points represent markers positioned on specific anatomical landmarks

- THI: Placed the marker over the lower lateral 1/3 surface of the thigh, just below the swing of the hand, although the height is not critical.
- ANK: Placed on the lateral malleolus along an imaginary line that passes through the transmalleolar axis
- TIB: Similar to the thigh markers, these are placed over the lower 1/3 of the shank to determine the alignment of the ankle flexion axis
- TOE: Placed over the second metatarsal head, on the mid-foot side of the equinus break between fore-foot and mid-foot
- HEE: Placed on the calcaneous at the same height above the plantar surface of the foot as the toe marker

In order to ensure the accuracy of the kinematic data, the placement of the markers was glued in the appropriate location by an experienced specialist before the start of the movement recording. All markers were fixed using special adhesive so that they would not be displaced during the execution of the movements. The subject appeared in the experimental environment wearing appropriate clothing and without any metallic or reflective objects on their clothing to avoid any disruption in data recording.

2.3.1. Modeling Assumptions

Musculoskeletal simulations were performed using OpenSim under standard assumptions. The generic Gait2392 model was scaled to the subject's anthropometry, assuming proportional segment geometry, fixed muscle attachments, and accurate marker placement, with soft tissue artifact not explicitly modeled (RMS marker error during scaling ≈1.1 cm, max ≈1.7 cm). Inverse kinematics assumed rigid segments and ideal joints (RMS ≈1.0 cm, max ≈3 cm). Inverse dynamics used rigid segments with predefined inertial properties and ideal joints. The Residual Reduction Algorithm (RRA) slightly adjusted segment masses and torso COM, reducing residual forces below 5% of body weight and residual moments within commonly reported ranges. Computed Muscle Control with internal static optimization estimated muscle forces assuming instantaneous activation, no fatigue, and deterministic recruitment, minimizing the sum of squared activations. These assumptions, together with the validation metrics, support the reliability of the predicted muscle forces.

2.4. Fatigue Protocol

After placing the markers at the designated locations, as described in a previous study [8], the participant was first asked to walk slowly along the specified path for one minute to record baseline data. Then, the participant walked on the treadmill at a speed of 3 kilometers per hour for 10 minutes. After that, to capture the movements, he walked again for one minute in front of the cameras. This process was repeated on the treadmill at speeds of 3.5, 4, and 4.5 kilometers per hour respectively, and after each 10-minute session, the participant walked for one minute on the chosen path in front of the cameras to record motion data. In the fifth stage, the participant walked on the treadmill at a speed of 6.5 kilometers per hour for 10 minutes, and finally, the cool-down phase included 5 minutes of walking at a slow pace. Therefore, the participant completed six distinct trials of walking continuously, without rest intervals between trials. At the conclusion of the protocol, the participant reported significant fatigue in certain lower limb muscles.

Due to the physical constraints of the laboratory, continuous recording of ground reaction force data was not possible; force data could only be recorded during steps when the foot was in contact with the force plates (Kistler Group, Switzerland, 1200 Hz): one plate (30 × 50 cm; model 9260AA3) and one plate (60 × 50 cm; model 9260AA6) (Fig. 4). The dimensions of the walking path were approximately 2.6 meters in length and 1.5 meters in width, and the force plates were installed as tiles embedded in the floor of the walking path (blue plates in Fig.4). The motion capture cameras (Vicon Motion Systems Ltd., UK, 120 Hz) were positioned to ensure full coverage of the walking path from multiple angles.

3. Results

To simulate the walking motion, all modeling steps outlined in Figure 1 were completed in OpenSim 4.1. The output of the Computed Muscle Control (CMC) stage provided estimates of muscle forces during each gait cycle of normal walking. The modeling process was based on trials in which the participant walked slowly along a predefined path. The selected muscles were those from various segments of the lower limb that are known to play significant roles in gait. A qualitative comparison between the estimated muscle force profiles and previously reported EMG signals of the same subject revealed broadly similar phase-dependent patterns across the gait cycle, with periods of increased and decreased muscle involvement occurring during comparable gait phases. The accuracy of the CMC simulations was evaluated using the knee flexion–extension position error (pErr). Across six trials, both RMS and maximum tracking errors for the left and right knees remained below 2° after conversion from radians to degrees, indicating accurate kinematic tracking.

RMS error was used to quantify the agreement between model predicted activations and experimentally recorded (Fig. 5). Both signals were normalized to 0–1 over the gait cycle. Similar approaches have been used previously to evaluate model validity [26] and RMS values in the lower range (e.g., 0.2–0.4) generally indicate better agreement between model output and EMG. The overall agreement between EMG and model-predicted activations was good (mean RMSE = 0.187 ± 0.084), with 98% of comparisons below 0.30. The largest discrepancy was observed for the left Soleus (RMSE = 0.34).

Fig 4: An image of the walking path, the location of the force plates (blue-colored plates), and the treadmill

Table 1 shows the average agreement between the activation results calculated in the CMC phase and the EMG of different muscles throughout the simulation. The muscles are ranked according to the root mean square error.

To quantitatively compare muscle performance between the healthy and injured leg, the Area Under the Curve (AUC) of the force generated by each muscle during each gait cycle was calculated separately for the right and left leg. The maximum AUC across all steps was determined for each muscle. Then, for each muscle, the difference in AUC between the right and left leg was computed for each step, representing the extent of muscle performance disparity between the two legs. To enable comparison across different muscles, all values were normalized to the maximum AUC of the respective muscle, resulting in a dimensionless and comparable index between muscles. This difference for various muscles is shown as a percentage of the maximum difference of the same muscle in Figure 6. The phases in this figure refer to the times when the subject walked slowly along a predetermined path.

The results are presented for four muscle groups of the lower limb in Fig. 6: a. the quadriceps femoris group, b. the hamstring muscle group, c. the posterior compartment (calf) muscles, and d. the other muscles of the leg. In these graphs, the solid-colored bars indicate greater force production in the left injured leg, while the patterned bars represent greater force production in the right leg.

Within the quadriceps muscle group, as shown in Fig. 6a, the Vastus Medialis and Vastus Intermedius muscles consistently produced greater force in the left leg compared to the right leg across all stages. This force difference reached up to a maximum of about 30%, whereas for the Rectus Femoris muscle, it did not exceed 15%. Moreover, in this muscle, the right leg generated greater force.

Greater differences were observed in the hamstrings, as shown in Fig. 6b. The Semimembranosus muscle exhibited a force production difference between the two legs ranging from 27% to 40% across all stages. For the Biceps Femoris, this difference ranged from 17% to 33%. The Semitendinosus muscle appeared to be somewhat more balanced, showing a difference between 2% and 25%.

As shown in Fig. 6c, the calf muscle group (both Gastrocnemius and Soleus) of the healthy leg had to produce more force than the injured leg. This was most significant in the Soleus muscle (with a difference ranging from 47 to 74%). The differences were smaller for the Gastrocnemius muscle, reaching a maximum of 27%.

As shown in Fig. 6d, among the other muscles of the Gracilis and Sartorius that were examined, the Sartorius muscle showed a difference in force production with a maximum of 20%, while this difference was significantly observed in the Gracilis muscle with a maximum of more than 45%. In both muscles, the left leg had to produce more force.

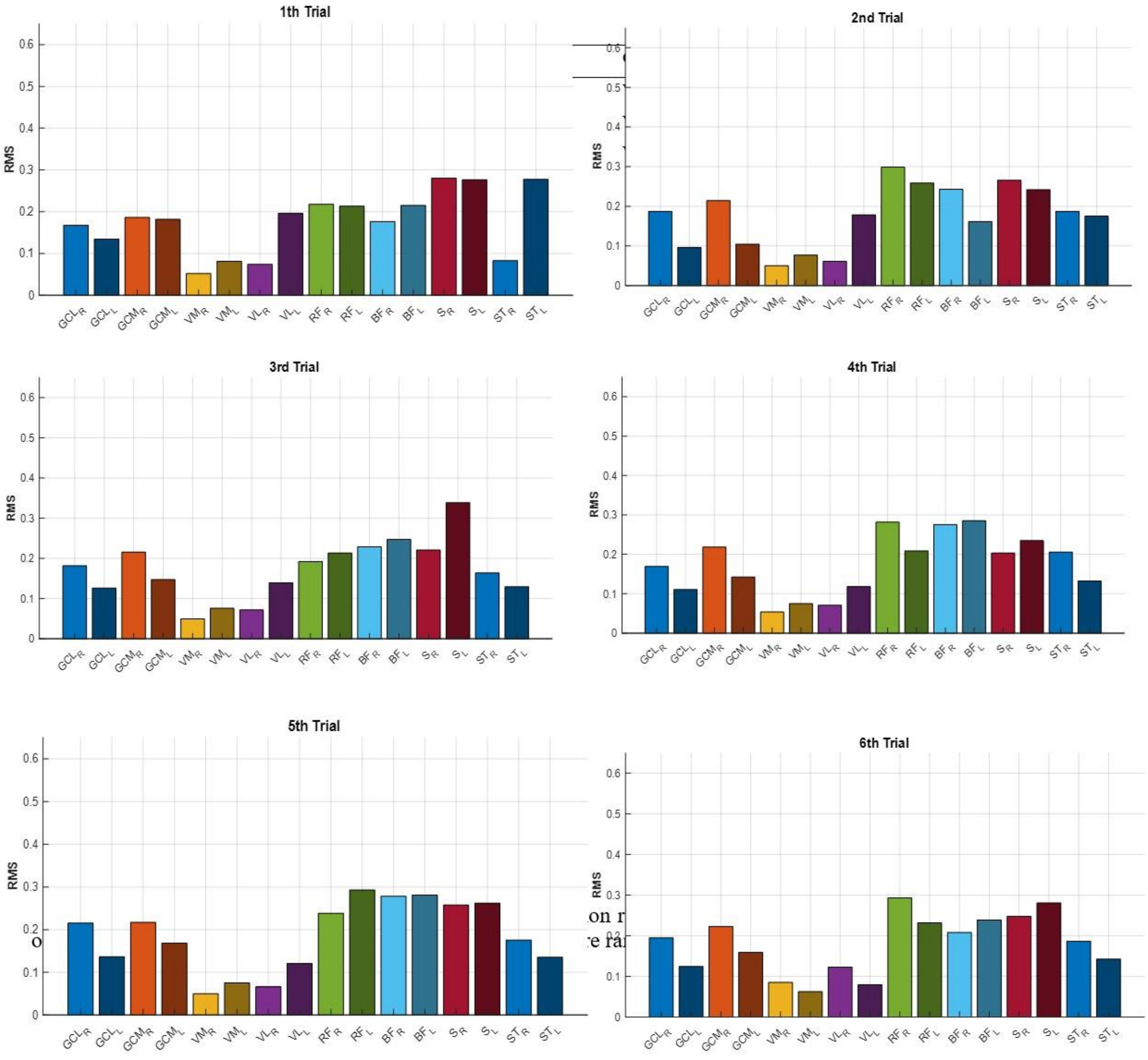

Fig 5: RMS error between model predicted activations and experimentally recorded EMG signals for 6 trials and 8 muscles of both legs

Table 1. The agreement between the activation in the CMC and the EMG of different muscles.

Muscle	Mean RMSE	Comment
Vastus Medialis (R)	0.06	Very good agreement
Vastus Medialis (L)	0.07	Very good agreement
Vastus Lateralis (R)	0.08	Very good agreement
Gastrocnemius Lateralis (L)	0.12	Good agreement
Vastus Lateralis (L)	0.14	Good agreement
Gastrocnemius Medialis (L)	0.15	Good agreement
Semitendinosus (L)	0.17	Low to moderate discrepancy
Semitendinosus (R)	0.17	Low to moderate discrepancy

Gastrocnemius Lateralis (R)	0.19	Low to moderate discrepancy
Gastrocnemius Medialis (R)	0.21	Low to moderate discrepancy
Biceps Femoris LH (R)	0.24	Moderate discrepancy
Biceps Femoris LH (L)	0.24	Moderate discrepancy
Rectus Femoris (L)	0.24	Moderate discrepancy
Rectus Femoris (R)	0.25	Moderate discrepancy
Soleus (R)	0.25	Moderate discrepancy
Soleus (L)	0.27	Largest amplitude difference

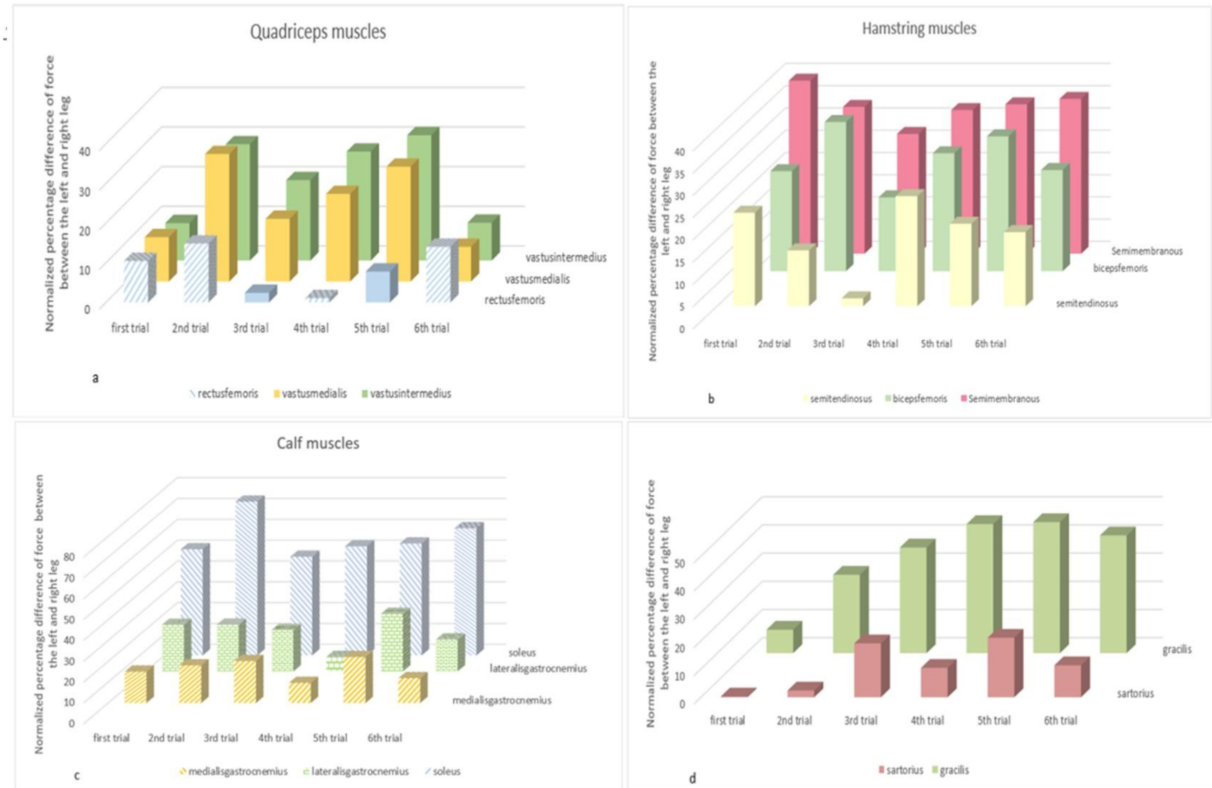

Fig 6: Normalized percentage difference in left (injured) and right (healthy) leg strength: a. Quadriceps muscles, b. Hamstring muscles, c. Calf muscles and, d. other muscles. The solid-colored bars indicate greater force production in the left injured leg, while the patterned bars represent greater force production in the right leg

4. Discussion

In this study, biomechanical modeling using OpenSim was employed to investigate changes in lower limb muscle function in an individual with an ACL rupture under conditions of repetitive activity and fatigue. Numerous studies have investigated individuals with ACL injury, primarily focusing on alterations in gait cycle patterns and lower limb muscle activity using electromyography signals. While EMG provides valuable information about neural activation, it does not directly quantify the forces generated by the muscles. To date, only a limited number of studies have attempted to estimate muscle forces in ACL-deficient subject [26] , and the effects of prolonged walking on muscle fatigue in this population remain largely unexplored. The present study addresses these gaps by employing musculoskeletal modeling to estimate muscle forces and examine fatigue-related changes during extended walking in an ACL-injured individual, providing novel insights into the neuromuscular adaptations associated with ACL deficiency. The results indicate that various muscles in the affected leg exhibit different performance patterns compared to the healthy leg. Furthermore, continuous activity-induced fatigue led to alterations in the force production patterns of the muscles. Previous studies have reported altered neuromuscular strategies in ACL-deficient individuals, with chronic, moderately active patients exhibiting altered muscle activation patterns and muscle force distribution during gait compared to healthy controls [27-29].

4.1. Quadriceps

In the quadriceps muscle group, the Vastus Medialis and Vastus Intermedius consistently generated greater force output in the injured leg compared to the unaffected leg throughout all phases of the study. This pattern suggests increased recruitment of these muscles in the injured leg, possibly as a compensatory response to anterior instability of the knee joint caused by ACL deficiency. This compensatory increase in vasti muscle activity is consistent with previous gait analyses in ACL-deficient individuals, which reported prolonged or altered quadriceps activation as a strategy to control tibial translation during stance phase [30]. However, this trend was not observed in the Rectus Femoris muscle, which did not demonstrate a consistent force pattern between the two legs. This finding has been demonstrated in another study, where the Rectus Femoris muscle force in the ACL-injured group was found to be lower than in the healthy limb [26]. Given that the Rectus Femoris is a biarticular muscle involved in both hip flexion and knee extension, its inconsistent activation may reflect altered motor control strategies or selective muscle coordination under fatigue conditions.

4.2. Hamstrings

In the hamstring muscle group, all three muscles—the Biceps Femoris, Semitendinosus, and Semimembranosus—generated lower forces in the right (healthy) leg compared to the left (injured) leg across all stages. This finding indicates that, in the absence of an intact anterior cruciate ligament, this muscle group compensates by producing greater force to fulfill its functional role. Previous musculoskeletal modeling studies have highlighted the differential contributions of lower limb muscles to ACL loading, demonstrating that quadriceps forces may increase anterior tibial shear, whereas hamstring forces can act protectively by reducing anterior tibial translation [18]. The increased hamstring force observed in the injured limb in the present study may therefore reflect a compensatory stabilization strategy. Such neuromuscular adaptations are likely critical for maintaining joint stability and controlling knee kinematics in the absence of ligamentous support. Among other important knee muscles, the Semimembranosus showed significant differences in force production between the two legs. This highlights the considerable impact of ACL injury on the hamstrings, substantially affecting their force-generating capacity.

4.3. Triceps Surae (Calf Muscles)

In contrast to the hamstring muscles, the triceps surae muscle group, —including the medial and lateral heads of the Gastrocnemius and the Soleus—generated greater forces in the right (unaffected) leg compared to the left (injured) leg throughout the testing stages. This observed increase in force production by the calf muscles in the unaffected leg which may reflect a compensatory strategy to maintain balance and propulsion during gait, especially given the impaired function of the injured leg. Previous studies have shown that gastrocnemius muscle force is reduced in ACL-deficient patients compared to healthy individuals, likely as an adaptation to limit anterior tibial translation, since the muscle acts as an ACL antagonist [26]. The Gastrocnemius and Soleus muscles play crucial roles in ankle plantarflexion and push-off phase of walking [16]. The Gastrocnemius is a biarticular muscle capable of generating both knee flexion and ankle plantarflexion moments. Its functions include plantarflexing the ankle when the knee is extended, raising the heel during walking, and flexing the leg at the knee joint. In contrast, the Soleus is a uniarticular muscle that produces only an ankle plantarflexion moment. Its role is to plantarflex the ankle regardless of the knee position and to stabilize the leg on the foot [16, 31]. Thus, greater force generation in the healthy leg could help stabilize the gait cycle and reduce load on the injured side. Poor performance of these muscles may result in decreased propulsion power and forward momentum during gait, potentially leading to compensatory or maladaptive movement patterns over time, which increase the risk of secondary injuries.

4.4. Other Muscles (Sartorius and Gracilis)

The Sartorius muscle in the right (unaffected) leg produced slightly less force compared to the left (injured) leg across most stages. In contrast, the Gracilis muscle in the injured leg generated substantially greater force than in the healthy leg. This pronounced asymmetry may indicate increased functional demand on the Gracilis, which, along with the Semitendinosus and Sartorius, contributes to dynamic stabilization of the knee through the pes anserinus group—especially in the absence of ACL integrity. The Gracilis is a thin and elongated muscle located on the medial side of the thigh, playing a crucial role in knee flexion and hip adduction [16]. Weakness or fatigue of this muscle in the injured leg can lead to reduced control during the swing phase of gait, where the knee must flex to allow the foot to lift off the ground and move forward. Additionally, due to its anatomical position, this muscle contributes to the medial stability of the knee.

4.5. Comparison with EMG Data

The results obtained in this study, when qualitatively and quantitatively compared with the ElectroMyoGraphy (EMG) data of the same patient reported in a previous article [8], in order to examine whether similar activation trends were observed. It should be noted that EMG signals represent neural activation and cannot be directly interpreted as muscle force.

Specifically, in the Vastus Medialis muscle, the EMG signals recorded from the left (injured) leg were notably higher than those from the right (healthy) leg, corroborating the musculoskeletal model's findings of increased force generation in these muscles on the injured side. In the posterior compartment of the lower leg, particularly within the Gastrocnemius lateralis and Soleus muscles, the right (healthy) leg demonstrated larger EMG signals, indicating greater muscle activation and force production compared to the injured limb which corresponds to EMG measurements. However, there are some mismatches between modeling and EMG measurements. Rectus Femoris, Biceps Femoris, and Semitendinosus force generations in the model is in opposite direction with respect to their behavior in EMG measurements.

4.6. Implications and Limitations

This study has several limitations:

1. the analysis was conducted on a single participant, which limits the generalizability of the findings. Inter-individual variability in musculoskeletal anatomy, muscle activation patterns, strength capacity, and movement strategies may influence muscle force estimations. Therefore, future studies including larger sample sizes are recommended to evaluate the generalizability and robustness of the present findings.
2. the musculoskeletal simulations were performed using the gait2392 model in OpenSim, which does not explicitly include knee ligaments such as the ACL. As a result, the mechanical consequences of ligament rupture were not directly modeled.
3. the knee joint is represented with simplified kinematics, potentially limiting the accuracy of estimated muscle forces under pathological conditions. These factors should be considered when interpreting the results.

The findings emphasize the need for caution when relying exclusively on modeling outputs, as the model did not incorporate all relevant physical constraints. For instance, the ACL rupture was not represented in the kinematic or dynamic analyses; only force plate reactions influenced muscle behavior. As a result, the small differences observed should be reexamined in an updated version of the model that explicitly accounts for ACL rupture. Nevertheless, the modeling approach offers valuable insights into deeper muscles that cannot be captured using surface EMG. Overall, these findings, combined with qualitative motion analysis, muscle activation timing, and muscle synergy patterns, can provide deeper insights into compensatory mechanisms and identify key intervention points in rehabilitation—especially during phases when individuals prepare to return to sports or daily activities. They highlight the complex neuromuscular adaptations that occur in response to the ACL injury and the compensatory mechanisms the body employs to preserve functional mobility. These force alterations appear to be compensatory responses to knee joint instability or suboptimal function of other muscles. Such compensatory mechanisms may develop to maintain knee stability, control unwanted movements, or redistribute load during different phases of the gait cycle. Therefore, these changes might reflect inefficient or energetically costly biomechanical strategies that, over time, could lead to fatigue, pain, or secondary injuries.

5. Conclusion

In conclusion, this study demonstrates that an ACL-deficient leg exhibits distinct compensatory patterns under fatigue, including:

- Increased force generation in quadriceps (Vastus Medialis and Intermedius) and hamstrings on the injured side.
- Increased calf muscle forces in the healthy leg, likely to stabilize gait and compensate for impaired injured-side function.
- Pronounced asymmetry in Gracilis and Sartorius, contributing to dynamic knee stabilization.

These findings complement previous EMG results and emphasize that muscle force adaptations are critical for preserving knee stability and functional mobility after ACL injury. They highlight the importance of considering muscle forces, not just surface EMG activity, when designing rehabilitation strategies. Future work should incorporate ligament dynamics into musculoskeletal models to better capture the mechanical effects of ACL deficiency and refine intervention strategies.

References

[1] H. Jebelli, J. Seo, S. Hwang, S. Lee, Physiology-based dynamic muscle fatigue model for upper limbs during construction tasks, *International Journal of Industrial Ergonomics,* Vol. 78, pp. 102984, 2020/07/01/, 2020.

[2] M. Elshafei, E. Shihab, Towards Detecting Biceps Muscle Fatigue in Gym Activity Using Wearables, *Sensors (Basel),* Vol. 21, No. 3, Jan 23, 2021. eng

[3] H.-W. Mueller-Wohlfahrt, L. Haensel, K. Mithoefer, J. Ekstrand, B. English, S. McNally, J. Orchard, C. N. van Dijk, G. M. Kerkhoffs, P. Schamasch, D. Blottner, L. Swaerd, E. Goedhart, P. Ueblacker, Terminology and classification of muscle injuries in sport: The Munich consensus statement, *British Journal of Sports Medicine,* Vol. 47, No. 6, pp. 342, 2013.

[4] B. E. Sibson, A. R. Harris, A. K. Yegian, A. Uwimana, A. Nuhu, A. Thomas, D. E. Anderson, R. M. Ojiambo, D. E. Lieberman, Associations of back muscle endurance with occupational back muscle activity and spinal loading among subsistence farmers and office workers in Rwanda, *PLOS ONE,* Vol. 19, No. 11, pp. e0309658, 2024.

[5] L. Ma, W. Zhang, B. Hu, D. Chablat, F. Bennis, F. Guillaume, Determination of subject-specific muscle fatigue rates under static fatiguing operations, *Ergonomics,* Vol. 56, No. 12, pp. 1889-1900, 2013/12/01, 2013.

[6] M. M. Eken, R. Richards, H. Beckerman, M. van der Krogt, K. Gerrits, M. Rietberg, V. de Groot, M. Heine, Quantifying muscle fatigue during walking in people with multiple sclerosis, *Clinical Biomechanics,* Vol. 72, pp. 94-101, 2020/02/01/, 2020.

[7] P. V. Viitasalo Jh Fau - Komi, P. V. Komi, Signal characteristics of EMG during fatigue, *European Journal of Applied Physiology and Occupational Physiology,* Vol. 37, No. 2, pp. 111-121, 1977/06/01, 1997. eng

[8] Z. Saghaeinooshabadi, M. R. Zakerzadeh, M. A. Nazari, The intricate link between anterior cruciate ligament rupture and lower limb muscle fatigue: a case study, *Eur J Orthop Surg Traumatol,* Vol. 35, No. 1, pp. 137, Mar 28, 2025. eng

[9] L. A.-O. Wang, Y. A.-O. X. Wang, A. Ma, G. Ma, Y. Ye, R. Li, T. A.-O. Lu, A Comparative Study of EMG Indices in Muscle Fatigue Evaluation Based on Grey Relational Analysis during All-Out Cycling Exercise, No. 2314-6141 (Electronic), 2018. eng

[10] J. Sun, G. Liu, Y. Sun, K. Lin, Z. Zhou, J. Cai, Application of Surface Electromyography in Exercise Fatigue: A Review, *Front Syst Neurosci,* Vol. 16, pp. 893275, 2022. eng

[11] K. Rostami, M. Alizadeh, H. Minoonejad, H. Yazdi, A. Thomas, Effect of Fatigue on Electromyographic Activity Patterns of the Knee Joint Muscles in Anterior Cruciate Ligament Reconstructed and Deficient Patients during Landing Task, *Journal of Functional Morphology and Kinesiology,* Vol. 3, pp. 22, 04/05, 2018.

[12] M. McHugh, T. Tyler, S. Nicholas, M. Browne, G. Gleim, Electromyographic Analysis of Quadriceps Fatigue After Anterior Cruciate Ligament Reconstruction, *The Journal of orthopaedic and sports physical therapy,* Vol. 31, pp. 25-32, 02/01, 2001.

[13] T. J. M. Dick, K. Tucker, F. Hug, M. Besomi, J. H. van Dieën, R. M. Enoka, T. Besier, R. G. Carson, E. A. Clancy, C. Disselhorst-Klug, D. Falla, D. Farina, S. Gandevia, A. Holobar, M. C. Kiernan, M. Lowery, K. McGill, R. Merletti, E. Perreault, J. C. Rothwell, K. Søgaard, T. Wrigley, P. W. Hodges, Consensus for experimental design in electromyography (CEDE) project: Application of EMG to estimate muscle force, *Journal of Electromyography and Kinesiology,* Vol. 79, pp. 102910, 2024/12/01/, 2024.

[14] C. Jing, W. Wang, D. Chablat, F. Bennis, *Evaluating the Risk of Muscle Injury in Football-Kicking Training with OpenSim*, in: Eds., pp. 100-109, 2021.

[15] A. Seth, M. Sherman, J. A. Reinbolt, S. L. Delp, OpenSim: a musculoskeletal modeling and simulation framework for in silico investigations and exchange, *Procedia IUTAM,* Vol. 2, pp. 212-232, 2011/01/01/, 2011.

[16] K. L. Moore, A. F. Dalley, A. M. R. Agur, *Chapter 5: Lower Limb*, in: *Clinically Oriented Anatomy*, Eds.: Lippincott Williams & Wilkins, 2009.

[17] C. L. Vaughan, Davis, B. L., and O'connor, J. C.,, 1992, *Dynamics of Human Gait, Human Kinetics*, Publishers Champaign, Illinois, United States,

[18] N. Maniar, M. H. Cole, A. L. Bryant, D. A. Opar, Muscle Force Contributions to Anterior Cruciate Ligament Loading, *Sports Med,* Vol. 52, No. 8, pp. 1737-1750, Aug, 2022. eng

[19] J. Moon, J. Lee, K. Kim, D. Koo, J. Lee, P. Pathak, G. A. Sanchez, S. B. Panday, Effect of Muscle-Specific Fatigue on the Risk of Anterior Cruciate Ligament Injury in Females, *Applied Sciences,* 11, 2021].

[20] A. Benjaminse, K. E. Webster, A. Kimp, M. Meijer, A. Gokeler, Revised Approach to the Role of Fatigue in Anterior Cruciate Ligament Injury Prevention: A Systematic Review with Meta-Analyses, *Sports Med,* Vol. 49, No. 4, pp. 565-586, Apr, 2019. eng

[21] *http://www.seniam.org/*, Accessed.

[22] S. L. Delp, F. C. Anderson, A. S. Arnold, P. Loan, A. Habib, C. T. John, E. Guendelman, D. G. Thelen, OpenSim: open-source software to create and analyze dynamic simulations of movement, *IEEE Trans Biomed Eng,* Vol. 54, No. 11, pp. 1940-50, Nov, 2007. eng

[23] *https://opensimconfluence.atlassian.net/*, Accessed.

[24] S. A. Roelker, E. J. Caruthers, R. K. Hall, N. C. Pelz, A. M. W. Chaudhari, R. A. Siston, Effects of Optimization Technique on Simulated Muscle Activations and Forces, *J Appl Biomech,* Vol. 36, No. 4, pp. 259-278, Aug 1, 2020. eng

[25] M. P. Kadaba, H. K. Ramakrishnan, M. E. Wootten, Measurement of lower extremity kinematics during level walking, *Journal of Orthopaedic Research,* Vol. 8, No. 3, pp. 383-392, 1990.

[26] H. Huang, W. Yin, S. Ren, Y. Yu, S. Zhang, Q. Rong, Y. Ao, Muscular Force Patterns during Level Walking in ACL-Deficient Patients with a Concomitant Medial Meniscus Tear, *Appl Bionics Biomech,* Vol. 2019, pp. 7921785, 2019. eng

[27] M. Lindström, L. Felländer-Tsai, T. Wredmark, M. Henriksson, Adaptations of gait and muscle activation in chronic ACL deficiency, *Knee Surg Sports Traumatol Arthrosc,* Vol. 18, No. 1, pp. 106-14, Jan, 2010. eng

[28] Q. Shao, T. D. MacLeod, K. Manal, T. S. Buchanan, Estimation of ligament loading and anterior tibial translation in healthy and ACL-deficient knees during gait and the influence of increasing tibial slope using EMG-driven approach, *Ann Biomed Eng,* Vol. 39, No. 1, pp. 110-21, Jan, 2011. eng

[29] E. S. Gardinier, K. Manal, T. S. Buchanan, L. Snyder-Mackler, Gait and neuromuscular asymmetries after acute anterior cruciate ligament rupture, *Med Sci Sports Exerc,* Vol. 44, No. 8, pp. 1490-6, Aug, 2012. eng

[30] Z. Knoll, R. M. Kiss, L. Kocsis, Gait adaptation in ACL deficient patients before and after anterior cruciate ligament reconstruction surgery, *J Electromyogr Kinesiol,* Vol. 14, No. 3, pp. 287-94, Jun, 2004. eng

[31] R. L. Lenhart, C. A. Francis, A. L. Lenz, D. G. Thelen, Empirical evaluation of gastrocnemius and soleus function during walking, *J Biomech,* Vol. 47, No. 12, pp. 2969-74, Sep 22, 2014. eng